Progress In Electromagnetics Research Letters, Vol. 82, 73–80, 2019

Coupling Matrix Optimization Synthesis for Filters with Constant and Frequency-Variant Couplings

Gang Li*

Abstract—This paper presents a quickly converging optimization technique for synthesis of filters with constant and frequency-variant couplings (FVC). Unlike the works so far appeared in the literature, the proposed technique is not based on the direct optimization of scattering parameters with assigned topology, but it consists of two procedures. Firstly, an FVC coupling matrix with assigned topology is suitably transformed by means of scaling and rotations for obtaining the new coupling matrix with constant couplings. Then, the cost function is constructed as a least squares problem involving both the eigenvalues of the new coupling matrix with constant couplings and that of the transversal coupling matrix. The solution is found via the solvopt optimization method. Two numerical examples with different topologies and specifications are synthesized to show the validation of the method presented in this paper.

1. INTRODUCTION

Modern wireless communication systems require complex filters with high performance and compact size. Synthesis techniques for such filters are one of the most researched topics in the field of high frequency electronics. Over the past few decades, a lot of efforts have been made for the direct synthesis of narrowband microwave filters. Basically, two topological configurations, namely cross-coupled [1–5] and extracted-pole [6–10], are introduced to generate finite transmission zeros (TZs) which are crucial to the performance of the filter. All of them assume that inter-resonator couplings are frequency-invariant. This assumption is true for a limited class of filters in a narrow frequency band. However, when the coupling structure of the filter has strong dispersion effect, which is explicit under broadband frequency condition, the frequency-invariant coupling coefficient usually does not reflect the actual behavior of the distributed coupling structure. The accuracy of the traditional coupling matrix synthesis method descends badly. Various researchers have demonstrated that taking into account frequency dependence of couplings allows generating additional transmission zeros. Combining cross-couplings with frequency-variant couplings allows reducing the overall number of couplings for a given set of transmission zeros. Moreover, it has been shown that frequency-variant couplings can generate transmission zeros in an in-line topology [11, 12]. But in [11], synthesis of the low-pass prototype for cross-coupled cavity filters with FVC has not been researched for more complex topologies. In [12], a general direct synthesis approach is presented for synthesizing in-line filters with multiple TZs. However, the number of TZs in [12] is $N/2$ (N is filter order). In [13], a general synthesis method for frequency-variant coupling matrix with user defined topology is presented. However, the approach in [13] cannot be applied to cross coupled filters with FVC which have multiple source-cavity couplings load-cavity couplings and direct source-load coupling. All the works in the literature [11–13] suffer from that there is no general synthesis technique allowing the design of filters including constant and frequency variant couplings with assigned topology.

Received 11 January 2019, Accepted 14 February 2019, Scheduled 12 March 2019
* Corresponding author: Gang Li (ligang@hbuas.edu.cn).
The author is with the School of Physics and Electronic Engineering, Hubei University of Arts and Science, Xiangyang 441053, China.

In order to overcome the mentioned drawbacks, we present, in this paper, a quickly converging optimization technique for synthesis of filters including constant and FVC with assigned topology. Compared with the synthesis approach in the literature [11–13], the method presented in this paper has following advantages: First, it is suitable for cross coupled filters with constant and FVC which have multiple source-cavity couplings and load-cavity couplings, even including direct source load couplings. Second, instead of directly optimizing coupling matrix with FVC, it optimizes the coupling matrix with constant couplings after matrix transformation, and the optimization is easy to converge. Third, with the direct source load coupling, the maximum number of TZs can be as many as the filter order N.

This paper is organized as follows. Basic theory on the coupling matrix transformation process is detailed in Section 2. In Section 3, two numerical examples with different topologies and specifications are synthesized to show the validation of the technique presented in this paper. Section 4 provides the conclusion.

2. BASIC THEORY

2.1. Matrix Transformation

The topology of cross coupled filters with constant and frequency-variant couplings is shown in Fig. 1. Generally, the inter-resonator coupling coefficients are frequency variant while the rest of the coupling coefficients are constant. In the normalized low-pass frequency domain, the nodal voltage equation of the network can be expressed as follows:

$$\left(-j\mathbf{G}+\mathbf{M}^0+\omega\mathbf{B}^1\right)\mathbf{V}=\mathbf{AV}=-j\mathbf{e} \tag{1}$$

where matrix $\mathbf{G}$ is of size $(N+2)*(N+2)$ with all its entries null except for the first and last diagonal elements which are equal to unity, $[\mathbf{G}]_{1,1}=[\mathbf{G}]_{N+2,N+2}=1$. Matrix $\mathbf{M}^0$ is of size $(N+2)*(N+2)$ with all its entries non-zero constants except for the first and last diagonal elements which are equal to null, $[\mathbf{M}^0]_{1,1}=[\mathbf{M}^0]_{N+2,\,N+2}=0$. ω is the normalized frequency. Matrix $\mathbf{A}=-j\mathbf{G}+\mathbf{M}^0+\omega\mathbf{B}^1$. The excitation vector is $\mathbf{e}=[10\ldots0]^T$. $\mathbf{V}$ is the node voltage column vector. Matrix $\mathbf{B}^1$ is an $(N+2)*(N+2)$ square matrix defined as follows:

$$\mathbf{B}^1=\begin{bmatrix} 0 & \ldots & 0 \\ \vdots & \mathbf{B} & \vdots \\ 0 & \ldots & 0 \end{bmatrix} \tag{2}$$

where matrix $\mathbf{B}$ is a square symmetric real matrix of size $N*N$ which is defined as:

$$\mathbf{B}=\begin{bmatrix} 1 & a_{12} & a_{13} & \ldots & \ldots & a_{1N} \\ a_{12} & 0 & a_{23} & \ldots & \ldots & a_{2N} \\ a_{13} & a_{23} & 1 & a_{34} & \ldots & \vdots \\ \vdots & \vdots & a_{34} & 1 & \ldots & \vdots \\ a_{1,N-1} & \ldots & \vdots & \ldots & 0 & a_{N-1,N} \\ a_{1N} & a_{2N} & \ldots & \ldots & a_{N-1,N} & 1 \end{bmatrix} \tag{3}$$

Element values on the principal diagonal of the matrix $\mathbf{B}$ imply different meanings. The element value 1 indicates that the node of the position corresponds to the resonator, while the value 0 corresponds to a non-resonant cavity. The other non-diagonal elements are generally non-zero constants, indicating frequency-variant couplings. According to the filter theory, S-parameters can be directly related to the coupling coefficients as follows:

$$\begin{cases} S_{11}=1+2j\left[\mathbf{A}^{-1}\right]_{1,1} \\ S_{21}=-2j\left[\mathbf{A}^{-1}\right]_{N+2,1} \end{cases} \tag{4}$$

where matrix $\mathbf{A}$ is given by $\mathbf{A}=-j\mathbf{G}+\mathbf{M}^0+\omega\mathbf{B}^1$. It is noted that the filter frequency response remain the same unless the elements of $\mathbf{A}^{-1}$ which appear in Eq. (4) are changed. Therefore, a series of scaling and similarity transformations can be performed on the coupling matrix with FVC. Without changing $[\mathbf{A}^{-1}]_{1,1}$ and $[\mathbf{A}^{-1}]_{N+2,1}$, the frequency-variant coupling elements of matrix $\mathbf{B}$ can be converted to

zero, and the frequency response of the filter remains unchanged. Based on matrix theory, any real and symmetric square matrix can always be diagonalized. The transformation matrix $\mathbf{T}$ is defined as follows:

$$\mathbf{T}=\begin{bmatrix} 1 & \dots & 0 \\ \vdots & \mathbf{U} & \vdots \\ 0 & \dots & 1 \end{bmatrix} \tag{5}$$

Matrix $\mathbf{U}$ is an $N*N$ square matrix containing normalized eigen-vectors of matrix $\mathbf{B}$. When matrix transformation is applied into Eq. (1), the following equations are obtained:

$$\begin{cases} \mathbf{G}^0_{new} = \mathbf{T}^T\mathbf{G}\mathbf{T}=\mathbf{G} \\ \mathbf{B}^1_{new} = \mathbf{T}^T\mathbf{B}^1\mathbf{T} \\ \mathbf{M}^0_{new} = \mathbf{T}^T\mathbf{M}^0\mathbf{T} \end{cases} \tag{6}$$

Obviously matrix $\mathbf{G}$ remains unchanged before and after matrix transformation. Matrix $\mathbf{B}^1_{new}$ is as follows:

$$\mathbf{B}^1_{new}=\begin{bmatrix} 0 & 0 & \dots & 0 & 0 \\ 0 & \Lambda_1 & 0 & 0 & 0 \\ \vdots & 0 & \ddots & 0 & \vdots \\ 0 & 0 & 0 & \Lambda_N & 0 \\ 0 & 0 & \dots & 0 & 0 \end{bmatrix} \tag{7}$$

where Λ_i is the eigenvalues of matrix $\mathbf{B}$. When $\mathbf{B}$ is a positive definite matrix, its eigenvalues are all positive. Eigenvalue Λ_i can be understood as the capacitance value of the filter network, which is the physical reason that $\mathbf{B}$ must be a positive definite matrix. Eq. (1) is transformed into the following form:

$$\left(-j\mathbf{G} + \mathbf{M}^0_{new} + \omega\mathbf{B}^1_{new}\right)\mathbf{V} = -j\mathbf{e} \tag{8}$$

Keep in mind that our aim is to transform Eq. (8) into the form:

$$\left(-j\mathbf{G} + \mathbf{M}^0_{final} + \omega\mathbf{B}^1_{final}\right)\mathbf{V} = -\,j\mathbf{e} \tag{9}$$

where matrix $\mathbf{B}^1_{final}$ is identical to $(N+2)*(N+2)$ identity matrix except for that $[\mathbf{B}^1_{final}]_{1,1} = [\mathbf{B}^1_{final}]_{N+2,\,N+2} = 0$. By multiplying the ith column and ith row of the matrix $(-j\mathbf{G} + \mathbf{M}^0_{new} + \omega\mathbf{B}^1_{new})$ by $1/\mathrm{sqrt}(\Lambda_i)$, we can get Eq. (9). This operation is mathematically equivalent to the transformation as follows:

$$\begin{cases} \mathbf{M}^0_{final} = \mathbf{S}\mathbf{M}^0_{new}\mathbf{S} \\ \mathbf{B}^1_{final} = \mathbf{S}\mathbf{B}^1_{new}\mathbf{S} \end{cases} \tag{10}$$

While the transformation matrix $\mathbf{S}$ is defined as follows:

$$\mathbf{S}=\begin{bmatrix} 1 & 0 & \dots & 0 & 0 \\ 0 & 1/\sqrt{\Lambda_1} & 0 & 0 & 0 \\ \vdots & 0 & \ddots & 0 & \vdots \\ 0 & 0 & 0 & 1/\sqrt{\Lambda_N} & 0 \\ 0 & 0 & \dots & 0 & 1 \end{bmatrix}$$

where Λ_i is the eigenvalues of matrix $\mathbf{B}$. It should be noted that the coupling matrix $\mathbf{M}^0_{final}$ is a matrix only with constant couplings, and the topology is totally different from the previous one with constant and frequency variant couplings.

2.2. Cost Function

According to the classical coupling matrix synthesis method [14], the transversal coupling matrix $\mathbf{M}_{trans}$ can be expressed as follows:

$$\mathbf{M}_{trans}=\begin{bmatrix} 0 & r_S^T & r_{SL} \\ r_S & \Lambda & r_L \\ r_{SL} & r_L^T & 0 \end{bmatrix} \tag{11}$$

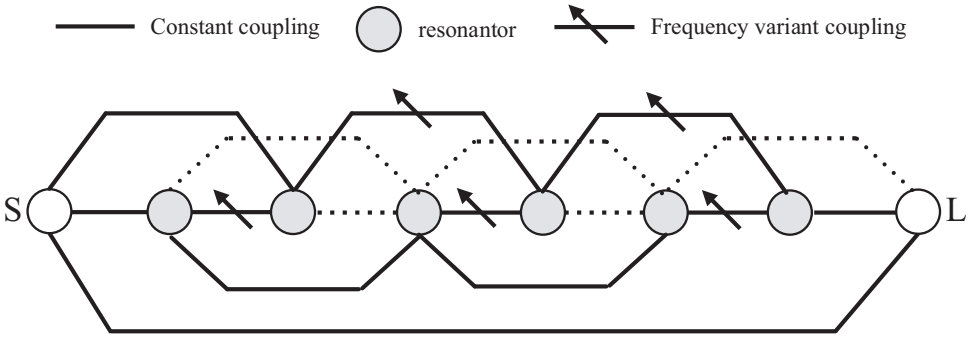

Figure 1. General topology of cross coupled filters with constant and frequency-variant couplings.

where Λ is a diagonal matrix, and r_{SL}, r_S^T, r_S, r_L, and r_L^T are non-zero constants. According to the filter theory, if the transformed coupling matrix $\mathbf{M}_{final}^0$ is similar to the transversal coupling matrix $\mathbf{M}_{trans}$, the corresponding frequency responses of the two coupling matrices are the same. So, the cost function is constructed as follows:

$$Cost = (\lambda_{trans} - \lambda_{final})^T(\lambda_{trans} - \lambda_{final}) \tag{12}$$

where $\lambda_{trans} = [\lambda_i^p; \lambda_i^{z1}; \lambda_i^{z2}; \lambda_i^c]$, where λ_i^p are the eigenvalues of the analytically synthesized transversal coupling matrix, λ_i^{z1} the eigenvalues of upper principal submatrix obtained by deleting the last row and column of the transversal matrix $\mathbf{M}_{trans}$, λ_i^{z2} the eigenvalues of lower principal submatrix obtained by deleting the first row and column of the transversal matrix $\mathbf{M}_{trans}$, and λ^c the eigenvalues of central submatrix obtained by deleting both the first and the last rows and columns of the transversal matrix $\mathbf{M}_{trans}$. λ_{final} is the vector of eigenvalues created in each iteration of the optimization routine. The element meaning of λ_{final} is the same as that of λ_{trans}. The minimization of the cost function can be performed using Solvopt algorithm [15]. The optimization flowchart is shown in Fig. 2.

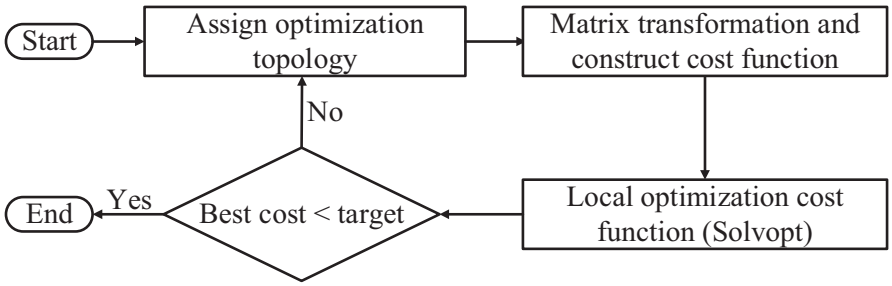

Figure 2. Optimization flowchart of the method presented in this paper.

3. EXPERIMENT RESULTS

For verification of the synthesis method presented in this paper, two examples are synthesized in this section. The initial values of optimization are random numbers whose values lie within specified limits $[-1, 1]$. The Solvopt algorithm uses numerical gradient, and the optimization process will terminate until the value of the cost function drops below 10^{-13}.

3.1. Example One

The first synthesized filter example is a fourth-order 20-dB return loss with different TZs numbers. There are four TZs located at $-3.2j$, $-2.1j$, $1.6j$ and $2.4j$. The topology is shown in Fig. 3(a), and the response is shown in Fig. 3(b).

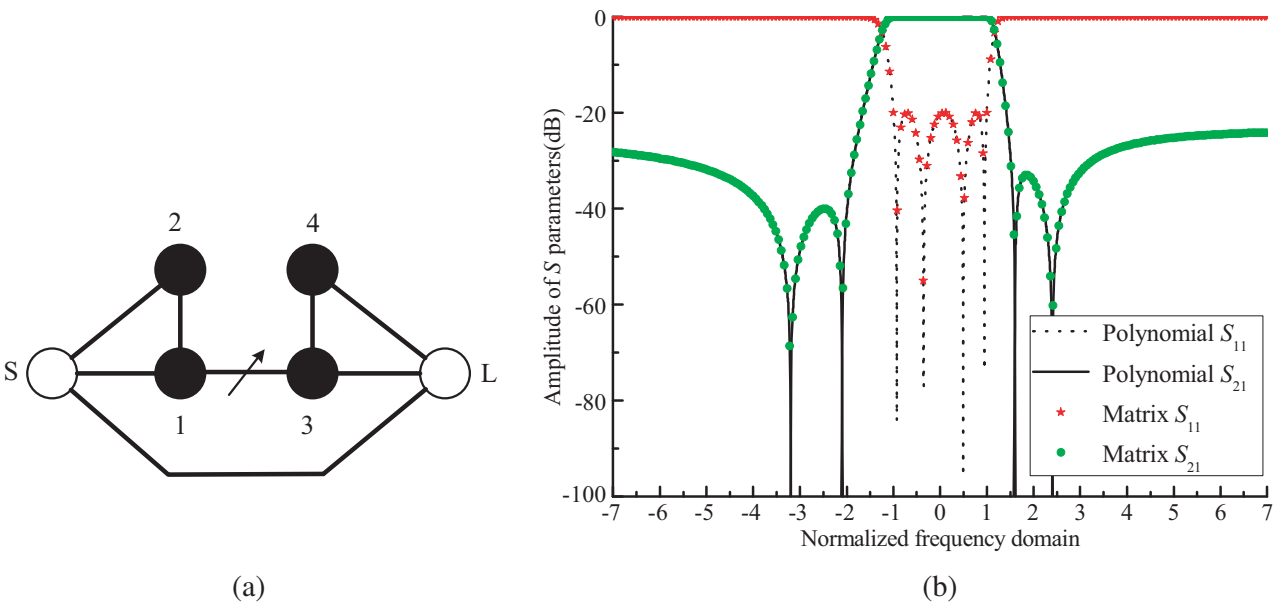

Figure 3. Topology and response of the filter. (a) Filter topology. (b) Filter response.

Using the method presented in Section 2, we obtain the coupling coefficients as follows.

$$\mathbf{M}^0 = \begin{bmatrix} 0 & 0.6519 & 0.7753 & 0 & 0 & -0.0309 \\ 0.6519 & 0.1951 & 0.4453 & -0.1252 & 0 & 0 \\ 0.7753 & 0.4453 & 0.9917 & 0 & 0 & 0 \\ 0 & -0.1252 & 0 & 0.4487 & -0.5895 & 0.5420 \\ 0 & 0 & 0 & -0.5895 & 0.9003 & 0.8570 \\ -0.0309 & 0 & 0 & 0.5420 & 0.8570 & 0 \end{bmatrix}$$

$$\mathbf{B}^1 = \begin{bmatrix} 0 & 0 & 0 & 0 & 0 & 0 \\ 0 & 1 & 0 & 0.7716 & 0 & 0 \\ 0 & 0 & 1 & 0 & 0 & 0 \\ 0 & 0.7716 & 0 & 1 & 0 & 0 \\ 0 & 0 & 0 & 0 & 1 & 0 \\ 0 & 0 & 0 & 0 & 0 & 0 \end{bmatrix}$$

The value of the cost function is $4.7949e-14$. The optimization time is less than 1.57 s. The polynomials response and matrix response agree well. Fig. 3(a) shows that coupling coefficient between resonator 1 and resonator 3 is frequency variant, and remaining coupling coefficients are constant. From Fig. 3(b), we can see that the number of TZs can be as many as the filter order.

3.2. Example Two

The second synthesized example is inline filters. The filter order is fifth-order. Return loss is 2-dB. Other specifications are shown as follows:

Prototype 1A: There are three TZs located at $-2.1j$, $1.6j$, and $2.4j$. The topology is shown as Fig. 4(a), and the response is shown in Fig. 4(b)

$$\mathbf{M}^0 = \begin{bmatrix} 0 & 0.9467 & 0 & 0 & 0 & 0 \\ 0.9467 & 0.6053 & 0.7934 & 0 & 0 & 0 \\ 0 & 0.7934 & -0.8126 & 0.7607 & 0 & 0 \\ 0 & 0 & 0.7607 & -0.1080 & 0.8789 & 0 \\ 0 & 0 & 0 & 0.8789 & -0.8273 & 0.9007 \\ 0 & 0 & 0 & 0 & 0.9007 & 0 \end{bmatrix}$$

$$\mathbf{B}^1 = \begin{bmatrix} 0 & 0 & 0 & 0 & 0 & 0 \\ 0 & 1 & 0.3306 & 0 & 0 & 0 \\ 0 & 0.3306 & 1 & -0.44417 & 0 & 0 \\ 0 & 0 & -0.4417 & 1 & 0.4185 & 0 \\ 0 & 0 & 0 & 0.4185 & 1 & 0 \\ 0 & 0 & 0 & 0 & 0 & 0 \end{bmatrix}$$

The value of the cost function is $3.3243e-14$. The optimization time is less than 1.03 s. The polynomials response and matrix response agree well. Fig. 4(a) shows that all inter-resonator coupling coefficients are frequency variant. From Fig. 4(b), we can see that the number of TZs equals number of frequency-variant couplings.

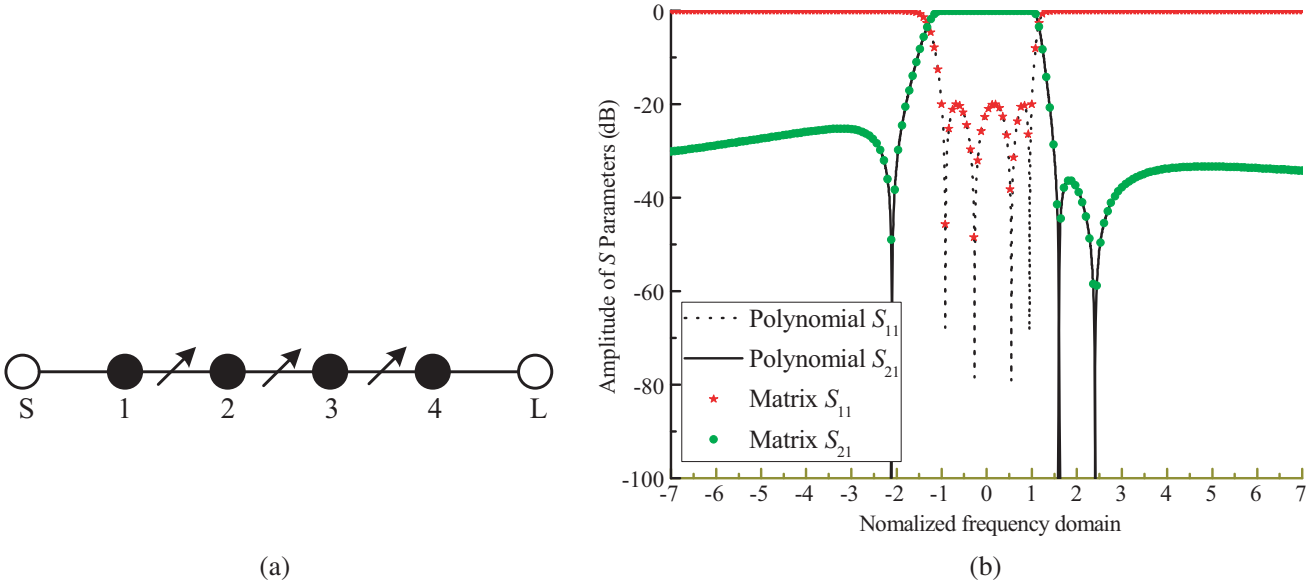

Figure 4. Topology and response of prototype 1A. (a) Filter topology. (b) Filter response.

Prototype 1B: There are four TZs located at $-2.1j$, $1.6j$, $2.4j$, and $-3.2j$. The topology is shown in Fig. 5(a), and the response is shown in Fig. 5(b)

$$\mathbf{M}^0 = \begin{bmatrix} 0 & 0.7753 & 0 & 0 & 0 & 0.0309 \\ 0.7753 & 0.9917 & 0.9790 & 0 & 0 & 0 \\ 0 & 0.9790 & -0.7351 & -0.4991 & 0 & 0 \\ 0 & 0 & -0.4991 & 0.4693 & -0.9794 & 0 \\ 0 & 0 & 0 & -0.9794 & 0.9003 & 0.8570 \\ 0.0309 & 0 & 0 & 0 & 0.8570 & 0 \end{bmatrix}$$

$$\mathbf{B}^1 = \begin{bmatrix} 0 & 0 & 0 & 0 & 0 & 0 \\ 0 & 1 & -0.6436 & 0 & 0 & 0 \\ 0 & -0.6436 & 1 & 0.0810 & 0 & 0 \\ 0 & 0 & 0.0810 & 1 & -0.5345 & 0 \\ 0 & 0 & 0 & -0.5345 & 1 & 0 \\ 0 & 0 & 0 & 0 & 0 & 0 \end{bmatrix}$$

The value of the cost function is $6.2969e-14$. The optimization time is less than 1.36 s. The polynomials response and matrix response agree well. Fig. 5(a) has one more sourceload coupling than Fig. 4(a). From Fig. 5(b), we can see that the number of TZs can be as many as the filter order. Comparing Fig. 3 and Fig. 5, it is noted that filter responses are the same, but the topologies are totally different.

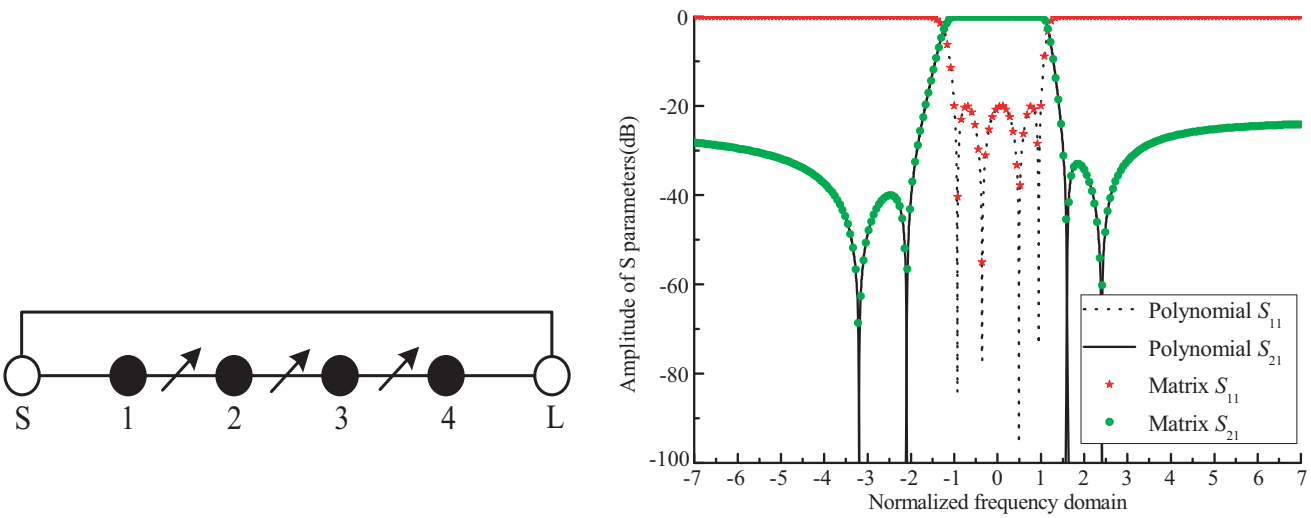

Figure 5. Topology and response of prototype 1B. (a) Filter topology. (b) Filter response.

4. CONCLUSION

An optimization synthesis approach for filter with constant and frequency-variant couplings is presented in this paper. Frequency-variant couplings (FVC) can generate and control multiple finite transmission zeros (TZs). It is valid for cross coupled filters with constant and frequency-variant couplings which have multiple source-cavity couplings and load cavity couplings, even including direct source-load coupling. Two examples with different topologies and specifications are synthesized to show the validation of the method presented in this paper. Although the analytical synthesis method is covered in this paper, further research work is needed to allow a wider practical use of these filters in the future.

ACKNOWLEDGMENT

This work was supported by the General Project Funding for Scientific and Technological Research in Xiangyang City in 2017.

REFERENCES

1. Amari, S., "Synthesis of cross-coupled resonator filters using an analytical gradient-based optimization technique," *IEEE Trans. Microw. Theory Techn.*, Vol. 48, No. 9, 1559–1564, Sep. 2000.
2. Cameron, R. J., C. Kudsia, and R. Mansour, "Coupling matrix synthesis of filter networks," *Microwave Filters for Communication Systems*, 1st Edition, Hoboken, NJ, USA, 2007.
3. Kozakowski, P., A. Lamecki, P. Sypek, and M. Mrozowski, "Eigenvalue approach to synthesis of prototype filters with source/load coupling," *IEEE Microw. Wireless Compon. Lett.*, Vol. 15, No. 2, 98–100, Feb. 2005.
4. Szydlowski, L., N. Leszczynska, and M. Mrozowski, "Dimensional synthesis of coupled-resonator pseudoelliptic microwave bandpass filters with constant and dispersive couplings," *IEEE Trans. Microw. Theory Techn.*, Vol. 62, No. 8, 1634–1646, Aug. 2014.
5. Gimenez, A. and D. Pedro, "A dual-TZ extraction technique for the synthesis of cross-coupled prototype filters," *IEEE Microw. Wireless Compon. Lett.*, Vol. 26, No. 10, 777–779, Oct. 2016.
6. He, Y., G. Wang, and L.-G. Sun, "Direct matrix synthesis approach for narrowband mixed topology filters," *IEEE Microw. Wireless Compon. Lett.*, Vol. 26, No. 5, 301–303, Apr. 2016.

7. Zhao, P. and K.-L. Wu, "A direct synthesis approach of bandpass filters with extracted-poles," *Proc. Asia-Pacific Microw. Conf.*, 25–27, Seoul, South Korea, Nov. 2013.
8. Yang, Y., M. Yu, and Q.-Y. Wu, "Advanced synthesis technique for unified extracted pole filters," *IEEE Trans. Microw. Theory Techn.*, Vol. 64, No. 12, 4463–4472, Dec. 2016.
9. He, Y., G. Wang, X.-T. Song, and L.-G. Sun, "A coupling matrix and admittance function synthesis for mixed topology filters," *IEEE Trans. Microw. Theory Techn.*, Vol. 64, No. 12, 4444–4454, Oct. 2016.
10. Tamiazzo, S. and G. Macchiarella, "Synthesis of cross-coupled prototype filters including resonant and non-resonant nodes," *IEEE Trans. Microw. Theory Techn.*, Vol. 63, No. 10, 3408–3415, Jul. 2015.
11. Amari, S. and U. Rosenberg, "Synthesis and design of novel in-line filters with one or two real transmission zeros," *IEEE Trans. Microw. Theory Techn.*, Vol. 52, No. 5, 1464–1478, May 2004.
12. He, Y., G. Macchiarella, G. Wang, W. Wu, L. Sun, L. Wang, and R. Zhang, "A direct matrix synthesis for in-line filters with transmission zeros generated by frequency-variant couplings," *IEEE Trans. Microw. Theory Techn.*, Vol. 66, No. 6, 1780–1789, Apr. 2018.
13. Szydlowski, L., A. Lamecki, and M. Mrozowski, "Coupled-resonator filters with frequency-dependent couplings: Coupling matrix synthesis," *IEEE Microw. Wireless Compon. Lett.*, Vol. 22, No. 6, 312–314, May 2012.
14. Cameron, R. J., "Advanced coupling matrix synthesis techniques for microwave filters," *IEEE Trans. Microw. Theory Techn.*, Vol. 51, No. 1, 1–10, Jan. 2003.
15. SolvOpt manual and SolvOpt Toolbox for matlab, Available: http://www.kfunigraz.ac.at/imawww/kuntsevich/solvopt/index.html.